



Synthesis of copper(II) and zinc(II) complexes with chalcone–thiosemicarbazone hybrid ligands: X-ray crystallography, spectroscopy and yeast activity

Igor Resendes Barbosa¹ · Isabela da Silva Pinheiro¹ · Alan Douglas Lopes dos Santos¹ · Aurea Echevarria¹ · Carla Marins Goulart¹ · Guilherme Pereira Guedes^{1,2} · Nathally Alves da Costa¹ · Beatriz Martinez de Oliveira e Silva¹ · Cristiano Jorge Riger¹ · Amanda Porto Neves¹

Received: 30 May 2018 / Accepted: 13 July 2018
© Springer Nature Switzerland AG 2018

Abstract

Four chalcone–thiosemicarbazones (C-TSCs) of the type 2-((*E*)-3-(4-**R**-phenyl)-1-phenylallylidene)-*N*-phenylhydrazinecarbothioamide, where **R** = Cl (**HL1**), NO₂ (**HL2**), CH₃ (**HL3**) or CN (**HL4**), were prepared in good yields from the reaction of the respective chalcone with 4-phenyl-3-thiosemicarbazide and HCl in EtOH. Reaction of HL with CuCl₂·2H₂O or ZnCl₂ in the presence of Et₃N afforded the complexes [M(L)₂], M = Cu(II) or Zn(II). X-ray diffraction analysis revealed that the ligands coordinate in their deprotonated form, in a bidentate fashion through the iminic nitrogen and sulfur atoms. Yeast activities of the compounds were tested, where the ligand **HL4** was the most damaging derivative, exhibiting cell viability at about 50%. On the other hand, lipid peroxidation assays revealed that the ligand **HL1** was able to better induce membrane damage compared to the other compounds. It has been found that coordination with Cu(II) and Zn(II) did not increase the biological activities of the C-TSCs.

Introduction

Thiosemicarbazones (TSCs) constitute a class of great interest in medicinal chemistry due to their important pharmacological properties, such as antitumor, antimicrobial, antiviral and antiparasitic activities [1]. They are also known for their excellent ability to chelate a wide variety of transition metals, moreover their coordination is usually associated with the improvement of their biological activities [2–4]. Zn(II) complexes of pyridine-TSCs showed greater antiproliferative activity compared to the free ligands, against MCF-7 (human

breast cancer), T24 (bladder cancer) and L929 (mouse fibroblast), with IC₅₀ values similar to or better than cisplatin, in the range of 0.35–6.40 μM [4].

Also, the chalcones (1,3-diaryl-2-propen-1-ones) represent important natural compounds which have received, along with their synthetic derivatives, considerable attention owing to their great range of bioactivities, such as anti-inflammatory, antimicrobial, antioxidant and anticancer properties [5]. Because of the presence of chalcone derivatives in different biologically active compounds, new compounds bearing this moiety have been extensively exploited.

In this context, chalcone-derived thiosemicarbazones have also been investigated as well as their metal complexes [6–9]. They have demonstrated potential activities like antimicrobial and cytotoxic. For instance, da Silva and colleagues [8] obtained a series of C-TSCs and its Cu(II) complexes whose cytotoxicity was tested against four tumor cell lines. Overall, the cytotoxicity significantly increased upon coordination, where the complexes exhibited very low IC₅₀ values, several of them at nanomolar concentrations.

A series of Zn(II) and Ga(III) complexes of C-TSCs have shown antimicrobial activity, where the Zn(II) compounds were more active than the ligands against one

Electronic supplementary material The online version of this article (<https://doi.org/10.1007/s11243-018-0262-0>) contains supplementary material, which is available to authorized users.

✉ Amanda Porto Neves
amandanevess@gmail.com

¹ Instituto de Química, Universidade Federal Rural do Rio de Janeiro, BR-465, Km 7, Seropédica, RJ CEP 23890-000, Brazil

² Present Address: Instituto de Química, Universidade Federal Fluminense, Campus do Valonguinho, Centro, Niterói, RJ CEP 24020-150, Brazil

bacteria strain. On the other hand, coordination to Ga(III) resulted in activity improvement of all C-TSC ligands [9].

Thiosemicarbazones can exist as thione–thiol tautomers and exhibit structural isomers (*Z* or *E*) in respect of the iminic nitrogen [10, 11]. In the complexes, they can bind to the metal either in neutral or in anionic form. Versatility of the TSCs allows the incorporation of different substituents that can increase the coordination sites of the derivatives, leading to complexes with different geometries, where the TSCs can act mainly as bidentate, tridentate or even tetradentate ligands [12]. It is known that minor structural modifications can affect the chemistry of the complex, and such knowledge is of crucial importance to understand their biological profiles. As it is well documented that the biological properties of C-TSC derivatives improve upon coordination to a transition metal, the present work aimed at synthesizing a new series of Cu(II) and Zn(II) complexes containing C-TSC ligands. In addition, toxicity of the compounds toward the model organism *Saccharomyces cerevisiae* has also been accessed.

Saccharomyces cerevisiae has become a useful and convenient model for studying the cytotoxic potential of synthetic drugs [13, 14]. Its resemblance to mammalian cells in relation to organelles, macromolecules and cellular structures has led to *S. cerevisiae* being one of the most common eukaryotic model systems used in studies related to cellular processes [15]. In addition, knowledge of the yeast genome allows genetic manipulations to obtain more sensitive strains to oxidative damage, such as the mutant deficient in glutathione synthesis ($\Delta gsh1$), which is a deficient strain in protection systems linked to the cells redox homeostasis [16].

Ligands and complexes have been also studied by spectroscopic methods, and the crystalline structures of the complexes were elucidated by X-ray diffraction analysis.

Experimental

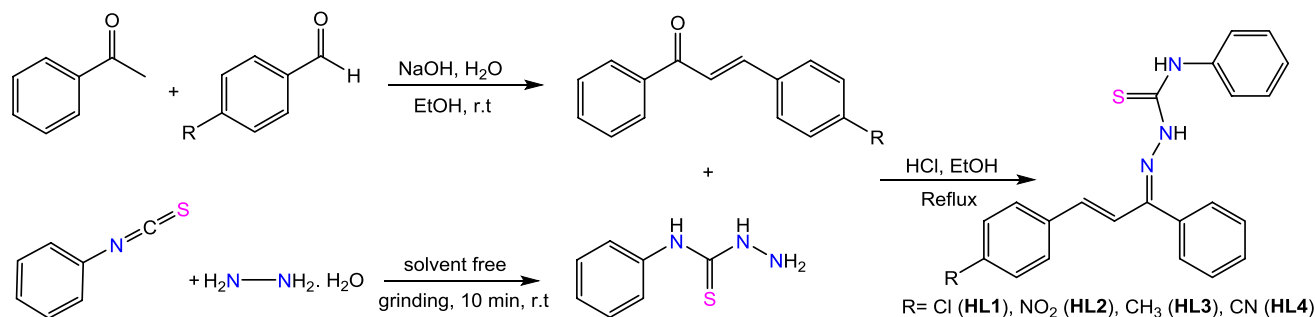
Materials and physical measurements

All commercial reagents and solvents were purchased from Aldrich and used without any further purification. The substituted chalcones (Scheme 1) were prepared according to the literature [17], and 4-phenyl-3-thiosemicarbazide was synthesized as described [18]. Phosphate buffer (pH 6.0) was prepared by dissolving 138 g of $\text{NaH}_2\text{PO}_4 \cdot \text{H}_2\text{O}$ and 142 g of Na_2HPO_4 in H_2O to a final volume of 1 L. The melting points were recorded on a PFM II capillary melting point apparatus. FTIR spectra were recorded on a FTIR Bruker Vertex 70 Spectrophotometer, using KBr pellets and scanned between 4000 and 600 cm^{-1} . Microanalyses were performed using a Perkin-Elmer CHN 2400 microanalyzer. Electronic spectra were recorded on a UV-1800 Shimadzu spectrophotometer with 1-cm quartz cells, using acetonitrile solutions of the compounds ($1.0 \times 10^{-5}\text{ mol L}^{-1}$) within the range 200–600 nm for the ligands and 200–900 nm for the complexes. ^1H (500 MHz) and ^{13}C NMR (125 MHz) spectra were carried out with a Bruker Ultrashield Plus in DMSO-d_6 (Tedia Brazil) containing tetramethylsilane as internal standard. Chemical shifts are reported in parts per million (ppm). Wild-type yeast strain BY4741 (*MATa*; *his3* $\Delta 1$; *leu2* $\Delta 0$; *met15* $\Delta 0$; *ura3* $\Delta 0$) was purchased from Euroscarf, Frankfurt, Germany.

Synthesis of the ligands

The substituted chalcone (2 mmol), 4-phenyl-3-thiosemicarbazide (0.501 g, 3 mmol) and drops of concentrated hydrochloric acid in 10 mL of ethanol were refluxed for 2–6 h. After cooling, the formed precipitate was filtered off and further recrystallized from ethanol. Scheme 1 shows the synthetic route.

2-((*E*)-3-(4-chlorophenyl)-1-phenylallylidene)-*N*-phenylhydrazinecarbothioamide, **HL1**.



Scheme 1 Synthetic route for the preparation of **HL1–HL4**

From 0.485 g of the respective chalcone. Yield 0.585 g, 75%; m.p. 159–160 °C. FTIR (KBr, cm^{-1}): 3306, 3209 and 3156 (N–H), 3051 and 2942 $\nu(\text{C–H}_{\text{vinyl}}/\text{C–H}_{\text{arom}})$, 1593 $\nu(\text{C}=\text{C}_{\text{vinyl}})$, 1519, 1482 and 1444 $\nu(\text{C}=\text{N}) + \nu(\text{C}=\text{C}_{\text{arom}})$, 980 $\nu(\text{C}=\text{C}_{\text{substituted trans}})$, 771 $\nu(\text{C}=\text{S})$. ^1H NMR (DMSO- d_6): Major isomer: δ 11.54 (s, N2–H), 10.06 (s, N3–H), 7.89 (d, $J=16.10$ Hz, H9), 7.84–7.14 (m, C–H_{arom}), 6.84 (d, $J=16.10$ Hz, H8). Minor isomer: 10.42 (s, N2–H), 9.03 (s, N3–H), 7.84–7.14 (m, C–H_{arom} + H9), 6.49 (d, $J=16.39$ Hz, H8). ^{13}C NMR (DMSO- d_6): Major isomer: 177.2 (C=S), 148.9 (C=N), 139.4, 138.9 (C9), 137.0, 135.3, 134.3, 130.2 (2C–H_{arom}), 129.9 (2C–H_{arom}), 129.7 (C–H_{arom}), 129.2 (2C–H_{arom}), 128.8 (2C–H_{arom}), 128.6 (2C–H_{arom}), 125.9 (2C–H_{arom}), 125.7 (C–H_{arom}), 120.1 (C8). Minor isomer: 139.2, 135.2, 133.7, 130.3, 129.8 (C–H_{arom}), 129.4 (C–H_{arom}), 129.1 (C–H_{arom}), 128.7 (C–H_{arom}), 125.5 (C–H_{arom}) 125.3 (C–H_{arom}). UV–Vis [CH_3CN ; λ/nm : 265, 343.

2-((*E*)-3-(4-Nitrophenyl)-1-phenylallylidene)-*N*-phenylhydrazinecarbothioamide, **HL2**.

From 0.506 g of the respective chalcone. Yield 0.660 g, 82%; m.p. 174–175 °C. FTIR (KBr, cm^{-1}): 3332, 3276 and 3213 (N–H), 3060 and 2936 $\nu(\text{C–H}_{\text{vinyl}}/\text{C–H}_{\text{arom}})$, 1595 $\nu(\text{C}=\text{C}_{\text{vinyl}})$, 1536, 1469 and 1441 $\nu(\text{C}=\text{N}) + \nu(\text{C}=\text{C}_{\text{arom}})$, 1340 (symmetrical N=O), 976 $\nu(\text{C}=\text{C}_{\text{substituted trans}})$, 789 $\nu(\text{C}=\text{S})$. ^1H NMR (DMSO- d_6): Major isomer: δ 11.65 (s, N2–H), 10.11 (s, N3–H), 8.29 (d, $J=8.91$ Hz, 2H_{arom}), 8.07–8.03 (m, C–H_{arom}), 8.04 (d, $J=16.14$ Hz, H9), 7.82–7.14 (m, C–H_{arom}), 6.98 (d, $J=16.14$ Hz, H8). Minor isomer: 10.49 (s, N2–H), 9.19 (s, N3–H), 8.23 (d, $J=8.91$ Hz, 2C–H_{arom}), 8.07–8.03 (m, C–H_{arom}), 7.82–7.14 (m, C–H_{arom} + H9), 6.64 (d, $J=16.42$ Hz, H8). ^{13}C NMR (DMSO- d_6): Major isomer: 177.3 (C=S), 148.1 (C=N), 147.8, 143.0, 139.4, 137.7 (C9), 136.8, 129.9 (2C–H_{arom}), 129.8 (C–H_{arom}), 129.4 (2C–H_{arom}), 128.8 (2C–H_{arom}), 128.6 (2C–H_{arom}), 126.0 (2C–H_{arom}), 125.8 (C–H_{arom}), 124.2 (2C–H_{arom}), 123.5 (C8). Minor isomer: 177.3 (C=S), 147.3, 142.9, 139.1, 130.6 (C–H_{arom}), 130.2 (C–H_{arom}), 128.7 (C–H_{arom}), 128.3 (C–H_{arom}), 125.4 (C–H_{arom}), 124.6 (2C–H_{arom}). UV–Vis [CH_3CN ; λ/nm : 274, 370.

2-((*E*)-3-(4-Tolyl)-1-phenylallylidene)-*N*-phenylhydrazinecarbothioamide, **HL3**.

From 0.444 g of the respective chalcone. Yield 0.505 g, 68%; m.p. 135–136 °C. FTIR (KBr, cm^{-1}): 3308 and 3157 (N–H), 3049 $\nu(\text{C–H}_{\text{vinyl}}/\text{C–H}_{\text{arom}})$, 2950 and 2916 $\nu(\text{C–H}_{\text{aliphatic}})$, 1597 $\nu(\text{C}=\text{C}_{\text{vinyl}})$, 1519, 1480 and 1444 $\nu(\text{C}=\text{N}) + \nu(\text{C}=\text{C}_{\text{arom}})$, 981 $\nu(\text{C}=\text{C}_{\text{substituted trans}})$, 779 $\nu(\text{C}=\text{S})$. ^1H NMR (DMSO- d_6): δ 11.48 (s, N2–H), 10.02 (s, N3–H), 7.86 (d, $J=16.07$ Hz, H9), 7.73–7.14 (m, C–H_{arom}), 6.80 (d, $J=16.07$ Hz, H8), 2.36 (s, CH₃). Minor isomer: 10.39 (s, N2–H), 8.94 (s, N3–H), 7.73–7.14 (m, C–H_{arom} + H9), 6.45 (d, $J=16.44$ Hz, H8), 2.31 (s, CH₃). ^{13}C NMR (DMSO- d_6): Major isomer: 177.1 (C=S), 149.5 (C=N),

140.6 (C9), 139.7, 139.4, 137.2, 133.6, 130.2 (C–H_{arom}), 129.9 (2C–H_{arom}), 129.7 (2C–H_{arom}), 128.8 (2C–H_{arom}), 128.6 (2C–H_{arom}), 128.5 (2C–H_{arom}), 127.3 (C–H_{arom}), 125.8 (2C–H_{arom}), 118.3 (C8), 21.5 (CH₃). Minor isomer: 139.2, 139.1, 133.5, 130.5 (C–H_{arom}), 130.0 (C–H_{arom}), 129.6 (C–H_{arom}), 128.7 (C–H_{arom}), 127.9 (C–H_{arom}), 125.7 (C–H_{arom}), 21.4 (CH₃). UV–Vis [CH_3CN ; λ/nm : 263, 340.

2-((*E*)-3-(4-Cyanophenyl)-1-phenylallylidene)-*N*-phenylhydrazinecarbothioamide, **HL4**.

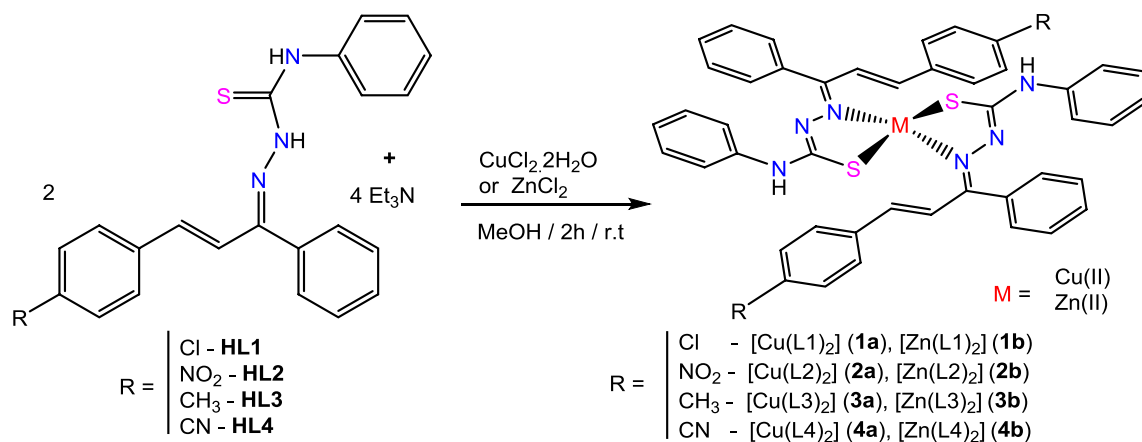
From 0.466 g of the respective chalcone. Yield 0.619 g, 81%; m.p. 176–177 °C. FTIR (KBr, cm^{-1}): 3334, 3278 and 3213 $\nu(\text{N–H})$, 3059, 2939 $\nu(\text{C–H}_{\text{vinyl}}/\text{C–H}_{\text{arom}})$, 2225 $\nu(\text{C}\equiv\text{N})$, 1596 $\nu(\text{C}=\text{C}_{\text{vinyl}})$, 1530, 1468 and 1439 $\nu(\text{C}=\text{N}) + \nu(\text{C}=\text{C}_{\text{arom}})$, 973 $\nu(\text{C}=\text{C}_{\text{substituted trans}})$, 795 $\nu(\text{C}=\text{S})$. ^1H NMR (DMSO- d_6): Major isomer: 10.46 (s, N2–H), 9.17 (s, N3–H), 7.99–7.19 (m, C–H_{arom}), 7.47 (d, $J=16.38$ Hz, H9), 6.56 (d, $J=16.38$ Hz, H8). Minor isomer: δ 11.60 (s, N2–H), 10.10 (s, N3–H), 8.00 (d, $J=16.11$ Hz, H9), 7.99–7.19 (m, C–H_{arom}), 6.91 (d, $J=16.11$ Hz, H8). ^{13}C NMR (DMSO- d_6): Major isomer: 177.3 (C=S), 148.3 (C=N), 141.0, 139.4 (C-1'''), 138.2 (C–H_{arom}), 136.8, 132.9 (2C–H_{arom}), 129.9 (2C–H_{arom}), 129.8 (C–H_{arom}), 129.1 (2C–H_{arom}), 128.8 (C–H_{arom}), 128.6 (2C–H_{arom}), 126.0 (2C–H_{arom}), 125.8 (C–H_{arom}), 122.7 (C8), 119.3 (CN), 111.5. Minor isomer: 140.9, 139.1, 135.1, 133.2 (C–H_{arom}), 132.5, 130.3, 128.7 (C–H_{arom}), 128.1 (C–H_{arom}), 125.5 (C–H_{arom}), 119.2 (CN), 111.1. UV–Vis [CH_3CN ; λ/nm : 266, 349.

Synthesis of the complexes [Cu(L1–4)₂] and [Zn(L1–4)₂]

Cu(II) and Zn(II) complexes were prepared from a general procedure illustrated in Scheme 2. To a suspension of the desired ligand **HL1–HL4** (0.12 mmol) in 3 mL of methanol was added Et₃N (0.033 mL, 0.24 mmol), followed by the addition of a previously prepared solution of the corresponding metal salt (0.010 g of CuCl₂·2H₂O or 0.008 g of ZnCl₂·0.06 mmol) in 2 mL of methanol. The resulting mixture was stirred at room temperature for 2 h and centrifuged, and the precipitate was washed with water and methanol and dried. Crude products were purified from diethyl ether by crystallization and dried in open air.

[Cu(L1)₂], **1a**. From 0.047 g of HL1. Yield 0.031 g, 61%; m.p. 140–142 °C. Anal. Calc. for C₄₄H₃₆Cl₂N₆S₂Cu · (CH₃CH₂)₂O: C, 62.7; H, 4.8; N, 9.1%. Found: C, 63.2; H, 5.0; N, 8.8%. FTIR (KBr, cm^{-1}): 3406 (N–H); 3055 and 2924 $\nu(\text{C–H}_{\text{vinyl}}/\text{C–H}_{\text{arom}})$, 1597 $\nu(\text{C}=\text{C}_{\text{vinyl}})$, 1526, 1495, 1475 and 1431 $\nu(\text{C}=\text{N}) + \nu(\text{C}=\text{C}_{\text{arom}})$. UV–Vis [CH_3CN ; λ/nm : 285, 323, 389.

[Cu(L2)₂], **2a**. From 0.048 g of HL2. Yield 0.040 g, 78%; m.p. 134–135 °C. Anal. Calc. for C₄₄H₃₆N₈O₄S₂Cu · 3/2 (CH₃CH₂)₂O: C, 61.4; H, 5.1; N, 11.5%. Found: C, 61.3; H, 5.2; N, 11.1%. FTIR (KBr, cm^{-1}): 3336 and 3277 (N–H);



Scheme 2 Synthesis of Cu(II) and Zn(II) complexes containing chalcone–thiosemicarbazone ligands

3056 and 2927 $\nu(\text{C-H}_{\text{vinyl}}/\text{C-H}_{\text{arom}})$, 1595 $\nu(\text{C}=\text{C}_{\text{vinyl}})$, 1517, 1495, 1470 and 1431 $\nu(\text{C}=\text{N}) + \nu(\text{C}=\text{C}_{\text{arom}})$, 1340 (NO_2). UV–Vis [CH_3CN]; λ/nm : 292, 308, 410.

[Cu(L3)₂], **3a**. From 0.044 g of HL3. Yield 0.041 g, 86%; m.p. 159–160 °C. Anal. Calc. for C₄₆H₄₂N₆S₂Cu · C₄H₄O: C, 68.8; H, 5.1; N, 9.6%. Found: C, 69.6; H, 5.0; N, 9.7%. FTIR (KBr, cm⁻¹): 3312 (N–H); 3053, 2921 and 2854 $\nu(\text{C-H}_{\text{vinyl}}/\text{C-H}_{\text{arom}})$, 1600 $\nu(\text{C}=\text{C}_{\text{vinyl}})$, 1530, 1498, 1478 and 1433 $\nu(\text{C}=\text{N}) + \nu(\text{C}=\text{C}_{\text{arom}})$. UV–Vis [CH_3CN]; λ/nm : 290, 327, 390.

[Cu(L4)₂], **4a**. From 0.046 g of HL4. Yield 0.035 g, 70%; m.p. 192–193 °C. Anal. Calc. for C₄₆H₃₆N₈S₂Cu · 1/2 CH₃OH: C, 66.3; H, 4.3; N, 13.3%. Found: C, 69.4; H, 4.3; N, 13.1%. FTIR (KBr, cm⁻¹): 3334 (N–H); 3053, 2971 and 2924 $\nu(\text{C-H}_{\text{vinyl}}/\text{C-H}_{\text{arom}})$, 2223 (C≡N), 1599 $\nu(\text{C}=\text{C}_{\text{vinyl}})$, 1528, 1494, 1468 and 1430 $\nu(\text{C}=\text{N}) + \nu(\text{C}=\text{C}_{\text{arom}})$. UV–Vis [CH_3CN]; λ/nm : 285, 404.

[Zn(L1)₂], **1b**. From 0.047 g of HL1. Yield 0.031 g, 61%; m.p. 200–201 °C. Anal. Calc. for C₄₄H₃₆Cl₂N₆S₂Zn · CH₃OH: C, 61.5; H, 4.4; N, 9.6%. Found: C, 61.6; H, 4.3; N, 9.4%. FTIR (KBr, cm⁻¹): 3332 (N–H); 3054, 2969 and 2923 $\nu(\text{C-H}_{\text{vinyl}}/\text{C-H}_{\text{arom}})$, 1596 $\nu(\text{C}=\text{C}_{\text{vinyl}})$, 1533, 1494, 1475 and 1430 $\nu(\text{C}=\text{N}) + \nu(\text{C}=\text{C}_{\text{arom}})$. ¹H NMR (400 MHz, DMSO-d₆): Major Z configuration: δ 9.92 (s, 1H, N3–H), 7.46 (d, $J = 16.05$ Hz, H9), 7.60–7.41 (m, C–H_{arom}), 7.34 (d, $J = 7.60$ Hz, C–H_{arom}), 7.27 (d, $J = 8.30$ Hz, C–H_{arom}), 7.16 (d, $J = 7.28$ Hz, C–H_{arom}), 6.97 (t, $J = 7.77$; 7.41; Hz, C–H_{arom}), 6.93–6.73 (m, C–H_{arom}), 6.65 (d, $J = 8.30$ Hz, C–H_{arom}), 6.59 (d, $J = 16.05$ Hz, H8). UV–Vis [CH_3CN]; λ/nm : 345, 356, 392.

[Zn(L2)₂], **2b**. From 0.048 g of HL2. Yield 0.031 g, 60%; m.p. 205–207 °C. Anal. Calc. for C₄₄H₃₆N₈O₄S₂Zn · CH₃OH: C, 60.0; H, 4.3; N, 12.5%. Found: C, 60.0; H, 4.2; N, 12.1%. FTIR (KBr, cm⁻¹): 3381, 3333 and 3276 (N–H); 3057 and 2925 $\nu(\text{C-H}_{\text{vinyl}}/\text{C-H}_{\text{arom}})$, 1595 $\nu(\text{C}=\text{C}_{\text{vinyl}})$, 1534, 1495, 1468 and 1428 $\nu(\text{C}=\text{N}) + \nu(\text{C}=\text{C}_{\text{arom}})$, 1340 (NO_2).

¹H NMR (400 MHz, DMSO-d₆): Major Z configuration: δ 10.06 (s, 1H, N3–H), 7.65 (d, $J = 15.82$ Hz, H9), 7.55–7.49 (m, C–H_{arom}), 7.45 (t, $J = 7.64$; 7.13 Hz, C–H_{arom}), 7.30 (d, $J = 7.95$ Hz, C–H_{arom}), 7.19 (d, $J = 7.13$ Hz, C–H_{arom}), 6.92 (t, $J = 7.95$; 7.45 Hz, C–H_{arom}), 6.72 (d, $J = 15.82$ Hz, H8). UV–Vis [CH_3CN]; λ/nm : 306, 393.

[Zn(L3)₂], **3b**. From 0.044 g of HL3. Yield 0.025 g, 53%; m.p. 210–212 °C. Anal. Calc. for C₄₆H₄₂N₆S₂Zn · H₂O: C, 67.0; H, 5.1; N, 10.2%. Found: C, 67.7; H, 5.0; N, 9.9%. FTIR (KBr, cm⁻¹): 3345 and 3346 (N–H); 3051, 3023 and 2918 $\nu(\text{C-H}_{\text{vinyl}}/\text{C-H}_{\text{arom}})$, 1602 $\nu(\text{C}=\text{C}_{\text{vinyl}})$, 1534, 1495, 1476 and 1429 $\nu(\text{C}=\text{N}) + \nu(\text{C}=\text{C}_{\text{arom}})$. ¹H NMR (400 MHz, DMSO-d₆): Major Z configuration: δ 9.82 (s, 1H, N3–H), 7.47 (d, $J = 15.62$ Hz, 1H, H9), 7.45–6.85 (m, C–H_{arom}), 6.54 (d, $J = 15.62$ Hz, 1H, H8), 6.57–6.46 (m, C–H_{arom}), 2.02 (s, 3H, CH₃). UV–Vis [CH_3CN]; λ/nm : 345, 355, 390.

[Zn(L4)₂], **4b**. From 0.046 g of HL4. Yield 0.038 g, 77%; m.p. 249–250 °C. Anal. Calc. for C₄₆H₃₆N₈S₂Zn · 1/2 CH₃OH: C, 66.1; H, 4.3; N, 13.3%. Found: C, 67.0; H, 4.3; N, 13.2%. FTIR (KBr, cm⁻¹): 3372 and 3338 (N–H); 3059, 2966 and 2923 $\nu(\text{C-H}_{\text{vinyl}}/\text{C-H}_{\text{arom}})$, 2222 (C≡N), 1599 $\nu(\text{C}=\text{C}_{\text{vinyl}})$, 1534, 1496, 1468 and 1428 $\nu(\text{C}=\text{N}) + \nu(\text{C}=\text{C}_{\text{arom}})$. ¹H NMR (DMSO-d₆): δ 10.01 (s, 1H, N3–H), 7.59 (d, $J = 15.81$ Hz, 1H, H9), 7.54 (t, $J = 7.78$, 7.53 Hz, 1H, C–H_{arom}), 7.48–7.39 (m, 4H, C–H_{arom}), 7.31 (d, $J = 8.03$ Hz, 2H, C–H_{arom}), 7.16 (d, $J = 7.53$ Hz, 2H, C–H_{arom}), 7.05–6.93 (m, 4H, C–H_{arom}), 6.90 (t, $J = 7.28$, 7.03 Hz, 1H, C–H_{arom}), 6.66 (d, $J = 15.81$ Hz, 1H, H8). UV–Vis [CH_3CN]; λ/nm : 285, 371, 401.

X-ray diffraction

Single-crystal X-ray data were collected on a Bruker D8 Venture diffractometer using graphite-monochromated Mo K α radiation ($\lambda = 0.71073$ Å) at room temperature (**1a**, **1b** and **4b**) and at 150 K for **3a**. Data collection, cell refinement

and data reduction were performed with Bruker Instrument Service v4.2.2, APEX2 [19] and SAINT [20], respectively. The absorption correction using equivalent reflections was performed with the SADABS program [21]. The structure solutions and full-matrix least-squares refinements based on F^2 were performed with the SHELXS-97 and SHELXL-2014 programs [22]. All atoms except hydrogen were refined anisotropically. Hydrogen atoms were treated using a constrained refinement. **1a** displayed large accessible voids, which are filled by disordered crystallization solvent molecules. As the efforts to assign these solvent intensities were unsuccessful, a solvent mask routine implemented in the Olex2 program was used [23]. The total volume of the voids and electrons per unit cell are 1761 Å³ and 442, respectively. The number of electrons per asymmetric unit corresponds to 55 ($Z=8$), which are in good agreement with one ethyl ether and one water as crystallization solvent. Structure drawings were generated using MERCURY program [24]. A summary of crystal structure, data collection and refinement for **1a**, **1b**, **3a** and **4b** is given in Table 1. Selected bond lengths and angles are listed in Table 2, while geometric parameters for hydrogen bonding and short contacts are gathered in Table 3.

Biological assays

Growth conditions

Cells were grown up to stationary phase in liquid YPD 2% medium (1% yeast extract, 2% glucose and 2% peptone), using an orbital shaker at 28 °C and 160 rpm, with the ratio of flask volume/medium of 5/1. Cellular density was determined by measuring the optical density of cell suspensions at 570 nm (OD_{570}) and converting to dry weight mL⁻¹ with a standard curve. Media components were obtained from BD Difco (USA). Stock solution of the compounds (0.002 g mL⁻¹) was prepared in water containing 50% DMSO.

Cell viability

Yeast cells were grown up to stationary phase (3.0 mg dry weight/mL), harvested by centrifugation and washed twice with 50 mmol L⁻¹ phosphate buffer (pH 6.0). Thereafter, cells (0.020 g) were resuspended in 20 mL of the same phosphate buffer containing 0.100 mmol L⁻¹ of the synthetic substances maintained at 28 °C/160 rpm for 4 h. The presence

Table 1 Summary of crystal data, collection and refinement parameters for **1a**, **1b**, **3a** and **4b**

Compound reference	1a	1b	3a	4b
Chemical formula	C ₄₄ H ₃₄ Cl ₂ CuN ₆ S ₂	C ₄₈ H ₄₂ Cl ₂ N ₆ OS ₂ Zn	C ₅₀ H ₄₈ CuN ₆ OS ₂	C ₄₆ H ₃₄ N ₈ S ₂ Zn
Formula mass	845.38	919.29	876.60	828.32
Crystal system	Orthorhombic	Triclinic	Triclinic	Monoclinic
Space group	<i>Pbcn</i>	<i>P</i> – 1	<i>P</i> – 1	<i>P2</i> ₁ / <i>n</i>
<i>a</i> /Å	18.7215(19)	10.5368(4)	10.4366(6)	13.9682(7)
<i>b</i> /Å	28.170(4)	14.7559(6)	14.5686(7)	15.8161(8)
<i>c</i> /Å	18.339(2)	15.2185(6)	15.8398(9)	19.6146(10)
α /°	90	91.301(2)	82.538(3)	90
β /°	90	101.699(2)	71.727(3)	108.592(2)
γ /°	90	95.566(2)	79.831(3)	90
Unit cell volume/Å ³	9672(2)	2303.91(16)	2243.9(2)	4107.2(4)
Temperature/K	293	293	150	293
<i>Z</i>	8	2	2	4
Radiation type	MoK α	MoK α	MoK α	MoK α
Absorption coefficient, μ /mm ⁻¹	0.68	0.78	0.62	0.74
No. of reflections measured	49,824	56,310	49,091	29,180
No. of independent reflections	8489	9460	9215	7560
R_{int}	0.061	0.086	0.11	0.058
Final R_1 values ($I > 2\sigma(I)$)	0.046	0.043	0.052	0.044
Final $wR(F^2)$ values ($I > 2\sigma(I)$)	0.113	0.083	0.117	0.091
Final R_1 values (all data)	0.079	0.086	0.096	0.084
Final $wR(F^2)$ values (all data)	0.147	0.098	0.139	0.112
Goodness of fit on F^2	1.19	1.01	1.04	1.05
Largest diff. peak/hole/e Å ⁻³	0.55/–0.56	0.29/–0.40	0.68/–0.58	0.43/–0.35
CCDC deposition	1835514	1835516	1835515	1835513

Table 2 Selected bond lengths (Å) and angles (°) for **1a**, **1b**, **3a** and **4b**

Atom labels	1a (M=Cu)	1b (M=Zn)	3a (M=Cu)	4b (M=Zn)
M–S1a	2.222(1)	2.2636(7)	2.226(1)	2.252(1)
M–S1b	2.232(1)	2.2529(9)	2.2293(9)	2.2493(9)
M–N1a	1.996(3)	2.068(2)	1.991(2)	2.072(3)
M–N1b	2.015(2)	2.041(2)	1.982(3)	2.060(2)
N1a–N2a	1.390(4)	1.381(3)	1.389(4)	1.383(3)
N1b–N2b	1.390(4)	1.384(3)	1.388(4)	1.380(3)
N2a–C16a	1.309(4)	1.301(3)	1.306(4)	1.311(5)
N2b–C16b	1.301(4)	1.304(4)	1.304(4)	1.311(4)
C16a–N3a	1.365(4)	1.360(3)	1.356(5)	1.360(4)
C16b–N3b	1.358(5)	1.362(3)	1.363(4)	1.367(4)
C16a–S1a	1.738(3)	1.754(2)	1.756(3)	1.744(3)
C16b–S1b	1.745(3)	1.757(3)	1.748(4)	1.753(3)
C8a–C9a	1.327(5)	1.330(4)	1.339(4)	1.336(5)
C8b–C9b	1.339(5)	1.334(4)	1.339(4)	1.336(4)
N1a–M–N1b	98.0(1)	104.96(8)	98.4(1)	101.8(1)
N1a–M–S1a	85.17(8)	86.41(6)	85.26(8)	87.06(7)
N1a–M–S1b	150.74(8)	122.85(6)	149.12(9)	125.32(7)
N1b–M–S1a	145.34(8)	128.29(6)	147.02(9)	127.47(7)
N1b–M–S1b	84.86(8)	87.64(6)	85.91(8)	87.66(7)
S1a–M–S1b	108.92(4)	128.25(3)	107.59(4)	128.55(4)
N1a–N2a–C16a–S1a	–0.9(4)	–2.3(3)	–0.5(4)	–0.3(4)
N1b–N2b–C16b–S1b	0.8(4)	1.9(4)	1.9(4)	1.5(4)

Table 3 Intermolecular and intramolecular contacts in **1a**, **1b**, **3a** and **4b** (values in Å and deg)

Compound	D–H...A	D–H	H...A	D...A	<D–H...A
1a	C22b–H22b...N2b	0.93	2.24	2.828(5)	120
	C18a–H18a...N2a	0.93	2.27	2.868(4)	121
1b	N3a–H3a...S1a ⁱ	0.86	2.84	3.411(2)	125
	N3b–H3b...O1s ⁱⁱ	0.86	2.05	2.907(3)	173
	C22a–H22a...N2a	0.93	2.30	2.871(4)	120
	C22b–H22b...N2b	0.93	2.29	2.868(3)	120
	C18b–H18b...Cl1a ⁱⁱⁱ	0.93	2.92	3.595(3)	131
	C8b–H8b...S1a	0.93	2.95	3.848(3)	162
3a	N3a–H3a...S1a ⁱ	0.88	2.61	3.456(3)	163
	N3b–H6b...O1s	0.88	2.05	2.930(4)	174
	C22a–H22a...S1a ⁱ	0.95	3.02	3.840(4)	145
	C18a–H18a...N2a	0.95	2.27	2.872(4)	121
	C8a–H8a...N1b	0.95	2.56	3.146(4)	120
	C8b–H8b...N1a	0.95	2.57	3.165(4)	121
	C18b–H18b...N2b	0.95	2.22	2.839(4)	122
4b	N3b–H3b...N4b ⁱ	0.86	2.32	3.179(4)	174
	N3a–H3a...S1a ⁱⁱ	0.86	2.82	3.426(3)	129
	C18a–H18a...N2a	0.93	2.26	2.847(4)	120
	C18b–H18b...N2b	0.93	2.31	2.865(4)	118

Symmetry codes: **1a** (i) $-x + 1, -y, -z + 1$; (ii) $x, y, z - 1$; (iii) $-x, -y + 1, -z$. **3a** (i) $-x + 1, -y + 1, -z + 1$. **4b** (i) $x, y - 1, z$; (ii) $-x + 2, -y + 2, -z + 2$

of DMSO did not influence the toxicity of the compounds since the percentage remained below 3% [25]. To test cellular tolerance against the substances, cells were diluted with water and plated on solid 2% YPD (1% yeast extract, 2% glucose, 2% peptone and 2% agar), after 4 h. Hydrogen peroxide was used as a positive control and the cells as the experimental control in phosphate buffer. Plates were prepared in triplicate. Colonies were counted after incubation at 28 °C for at least 72 h. Tolerance was expressed as a percentage of viable cells [26]. Assays were repeated three independent times.

Lipid peroxidation levels

Lipid oxidation was measured by TBARS (thiobarbituric acid-reactive species) method, which detects malondialdehyde (MDA). Cells (0.050 g-dry weight) were resuspended in 20 mL of the phosphate buffer containing 0.100 mmol L⁻¹ of the synthetic substances kept at 28 °C/160 rpm for 4 h. Hydrogen peroxide was used as a positive control at the same concentration, and the cells were tested in phosphate buffer as the experimental control. Cells were harvested by centrifugation and washed twice with phosphate buffer. The pellets were resuspended in 0.5 mL of the same buffer, followed by 10% trichloroacetic acid, and then 1.5 g of glass beads was added. The samples were lysed by 6 cycles of 20-s agitation on

a vortex mixer, followed by 20 s on ice. Extracts were centrifuged (4000 rpm/4 min) and the supernatant mixed with 0.1 mL of EDTA 0.1 mol L^{-1} and 0.6 mL of TBARS 1% (w/v), prepared in NaOH 0.05 mol L^{-1} . The reaction mixture was incubated in a boiling water bath for 15 min, and after cooling, the absorbance was measured spectrophotometrically at 532 nm. The results are expressed as pmol MDA/mg cell [26]. Assays were repeated three independent times.

Results and discussion

The proligands were prepared using an adapted methodology [27] from a mixture of previously synthesized substituted chalcones [17] and phenyl-thiosemicarbazide [18] using few drops of concentrated HCl in ethanol. The products were purified by recrystallization from ethanol in reasonable yields (68–82%). All metal complexes were obtained in 2:1 (ligand:metal) proportion using excess of Et_3N in a suspension of the desired ligand to allow deprotonation. After adding the metal salt, the complexes precipitated immediately as brownish green, orange and yellow solids, which were obtained in pure form by crystallization from the diethyl ether solutions and confirmed by elemental analysis. All complexes are poorly soluble in polar organic solvents such as methanol, ethanol and CH_3CN .

Suitable single-crystals for X-ray diffraction were obtained by slow evaporation of the solutions of **3a** and **1b** in methanol–THF (1:1). **4b** crystals were obtained in methanol–acetone (1:1) and **1a** in diethyl ether.

Vibrational spectra

The IR spectra of the chalcone–thiosemicarbazones exhibit the characteristic $\nu(\text{NH})$ stretching vibrations in the $3334\text{--}3156 \text{ cm}^{-1}$ range. For the complexes, the absence of the least energetic NH band at about 3200 cm^{-1} confirmed deprotonation of the thioamide NH function and coordination of the ligand in the anionic form [28]. The band around 1595 cm^{-1} attributed to the vinyl $\nu(\text{C}=\text{C})$ was not shifted upon complexation, as expected. A significant change was observed in the bands associated with the $\nu\text{C}=\text{C}_{\text{Ar}} + \nu\text{C}=\text{N}$, found in the range of $1545\text{--}1440 \text{ cm}^{-1}$ for **HL1–HL4** and shifted to $1535\text{--}1430 \text{ cm}^{-1}$ after coordination. In addition, a new intense absorption at about 1595 cm^{-1} appeared in the spectra of the complexes, confirming coordination through the iminic nitrogen [29]. **HL4**, **4a** and **4b** have the $\nu(\text{C}\equiv\text{N})$ assigned at 2224 cm^{-1} . Finally, **HL2**, **2a** and **2b** display an intense band at 1340 cm^{-1} characteristic of nitro group.

^1H NMR spectroscopy

The free proligands show the characteristic NH signals (N2–H and N3–H) within the range 10.4–11.7 and 9.0–10.1 ppm, respectively. The $=\text{C}\text{--}\text{H}$ (H8 and H9) appear in the regions of 6.5–7.0 and 7.4–8.1 ppm, respectively, as duplets with coupling constants of 16 Hz, characteristic of *trans* configuration. Aromatic hydrogens were all found between 7 and 8 ppm, as expected.

Duplicated peaks in the spectra of all proligands are observed, such as H8, H9, N2–H, N3–H and the $-\text{CH}_3$ group (H23–**HL3**), indicating the presence of two isomers in solution (1:3 proportion, see for **HL4**, Fig. 1). The literature reports the possibility of formation of *E* and *Z* isomers for similar chalcone–thiosemicarbazone compounds [9] that depends on the R-substituent of the chalcone as well as how long the substances remain in solution. Figure 1 illustrates the comparison between the ^1H NMR spectra of **HL4** and its Zn(II) complex, **4b**.

After coordination, the N2–H in the spectra of **4b** disappeared, confirming the anionic form of the thiosemicarbazone ligands. H9, H10 and aromatic hydrogens were found in the characteristic regions.

It is interesting to note individual signals for each hydrogen in the spectra of **4b**, implying the presence of one isomer in solution. However, the ^1H NMR spectra of the other Zn complexes (**1b–3b**) exhibited some duplicated peaks in a very small amount ($\sim 10\%$), which possibly might be related to traces of the other isomer in solution. According to the X-ray structures of **1a**, **1b**, **3a** and **4b**, all complexes exhibited the ligands in the *Z*-configuration, where the phenyl ring of the C7=N1 bond is orientated toward the thiosemicarbazone group. Thus, the *Z*-isomer must be the most stable form for the complexes both in the solid state and in solution.

Electronic spectra

The electronic spectra of the proligands show very similar profiles, with two main absorptions around 270 nm and in the 340–370 nm range. The first transition of medium intensity has been attributed in the literature as $\pi\text{--}\pi^*$ transitions of the aromatic rings [8, 9]. The most energetic absorption at 340–370 nm has been usually assigned as $n\text{--}\pi^*$ bands from the azomethine and thioamide functions [8]. As pointed out in the literature, it is also possible that these intense absorptions are a result of both $\pi\text{--}\pi^*$ and $n\text{--}\pi^*$ transitions overlapped in the same envelope [9]. The Cu(II) complexes exhibit two broad bands from 285 to 320 nm that can be assigned as ligand $\pi\text{--}\pi^*$ transitions. The presence of a new absorption around 389–410 nm could be associated with the shift of the $n\text{--}\pi^*$ transitions attributed to C=N and C=S upon coordination and the formation of higher conjugated system after deprotonation of the ligands [9]. Some studies

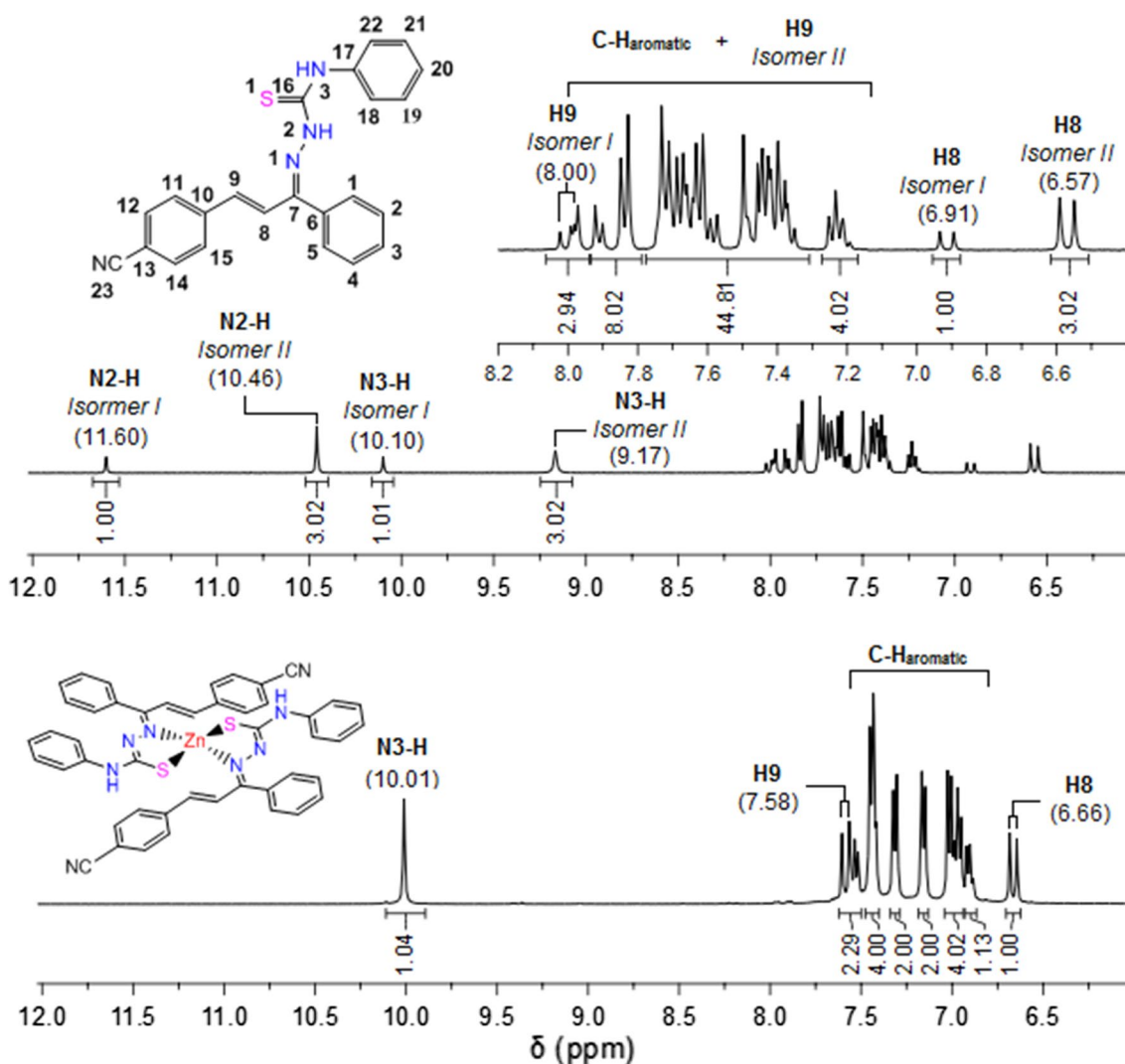


Fig. 1 ^1H NMR spectra of **HL4** and its Zn complex, in DMSO-d_6 , from 6.0 to 12.0 ppm

also suggest that these bands may be probably overlapped with ligand-to-metal charge transfer (LMCT) transitions [8]. The presence of the Cu(II) has been confirmed by the characteristic broad $d-d$ transitions around 610 nm, from the concentrated solutions. For the Zn(II) complexes, the $\pi-\pi^*$ and $n-\pi^*$ transitions of the ligands have been shifted after coordination, appearing as broad bands in the 343–370 and 391–421 nm ranges, toward the visible region, as expected.

Crystal structure descriptions

Suitable single-crystals for X-ray diffraction of the complexes **1a**, **1b**, **3a** and **4b** were obtained by slow solvent evaporation at 10 °C. A summary of crystal data, collection and refinement parameters is listed in Table 1. Selected bond lengths and angles are gathered in Table 2. Figure 2a–d

displays the asymmetric unit of all compounds with main atom numbering.

In all complexes, two chalcone-thiosemicarbazonate ligands (L^-) are coordinated to the metal in a bidentate mode via the azomethine nitrogen (N1a and N1b) and the S-thiolate (S1a and S1b) atoms, leading to a 5-membered chelate. The deprotonation of the thiosemicarbazone moieties was confirmed by the double-bond character of N2a–C16a, N2b–C16b, N1a–C7a, N1b–C7b, which present lengths around 1.30 Å. Besides, the C16a–S1a and C16b–S1b bond lengths are in the range 1.738(3)–1.757(3) Å, also supporting the evidence of the thiolate formation. The metal atoms are four-coordinated, and the complexes exhibit a seesaw geometry, determined by the calculation of τ_4 parameter [30] (**1a** 0.45; **1b** 0.73; **3a** 0.45; and **4b** 0.73). The M–N and M–S bond lengths are typical when compared to other compounds previously reported [3, 10], being slightly shorter

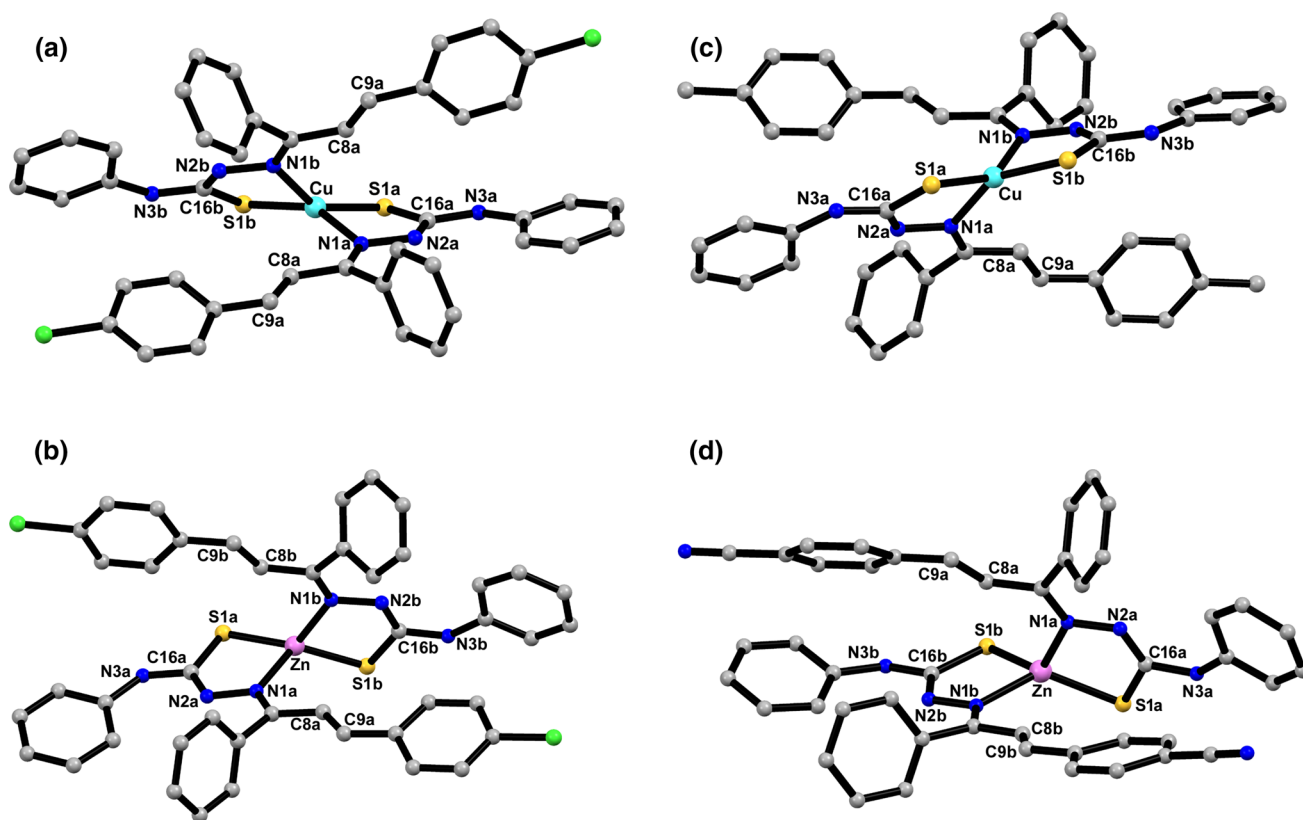


Fig. 2 Crystal structures of compounds **1a** (a), **1b** (b), **3a** (c) and **4b** (d). Hydrogen atoms and solvent molecules are omitted for the sake of clarity. Color codes: C (gray), N (blue), S (yellow), Cl (green), Zn (magenta) and Cu (cyan). (Color figure online)

for the Cu(II) complexes. Both ligands in the coordination sphere adopt the *ZZ*-configuration with respect to the C7a–N1a and C16a–N2a or C7b–N1b and C16b–N2b bond pairs. It is important to stress that the *Z*-orientation related to the C16a–N2a and C16b–N2b bonds is required to allow the simultaneous coordination from sulfur and nitrogen atoms. In the compounds **1a** and **3a**, both phenyl rings on the C7a or C7b are orientated almost perpendicular to the respective five-membered rings containing the metal atom with angles of 79.689(2)° and 78.162(2)° (**1a**, 86.022(1)° and 79.890(8)° **3a**). It was observed that these angles are closer for other compounds with values of 60.904(9)° and 83.365(9)° (**1b**) and from 64.940(1)°–72.314(1)° (**4b**). The orientation of the phenyl rings attached to C7a or C7b atoms seems to generate less steric effect, once both R-Ph group and NH-Ph are in opposite sites. Concerning the NH-Ph moiety, the phenyl ring is coplanar to the C16–N2–N1–C7 skeleton (a and b ligands) in all compounds and this is attributed to the establishment of intramolecular hydrogen bonds N–H···H–Csp₂, as exemplified in Fig. 3a for **1a**.

A short intermolecular S1b···S1bⁱ ($i = -x, y, 1/2 - z$) contact was observed only in **1a** with distance of 3.358(1) Å and the angles between the axes that pass through the middle of the C–S–Cu moiety of each fragment and the

intermolecular S···S bond (θ and ϕ) of 130°. These geometry parameters lie on the typical ranges found in the literature (S···S = 3.4–4.3 Å and $\theta, \phi = 90^\circ$ –140°) [31]. The R-substituent plays a key role in the crystal packing of the compounds due to intermolecular short contacts between the main molecular units and the crystallization solvents. For **1b**, **3a** and **4b**, the face-to-face molecular synthons involving azomethine hydrogen atom and the neighboring sulfur atom lead to supramolecular dimers, which interact with each other through Csp₂–H···Cl (**1a**), Csp₂–H···S (**3a**) weak contacts or NH···N_{cyno} hydrogen bonds (**4b**) (Fig. 3b, c).

Biological assays

The toxicity of the ligands **HL1**, **HL3** and **HL4** and the complexes **1a**, **3a**, **4a**, **1b**, **3b** and **4b** was evaluated toward *S. cerevisiae* cells (control strain—BY4741) after 4-h incubation at 100 μM (Table 4). **HL2**, **2a** and **2b** were not tested due to low solubility.

The results have shown that **HL4** was the most damaging compound, resulting in a cell viability of 53.53 ± 14.21%, while **HL1** and **HL3** showed lower toxicity. It has been reported in the literature that thiosemicarbazone derivatives exhibit toxicity against microorganisms such as *S. cerevisiae*

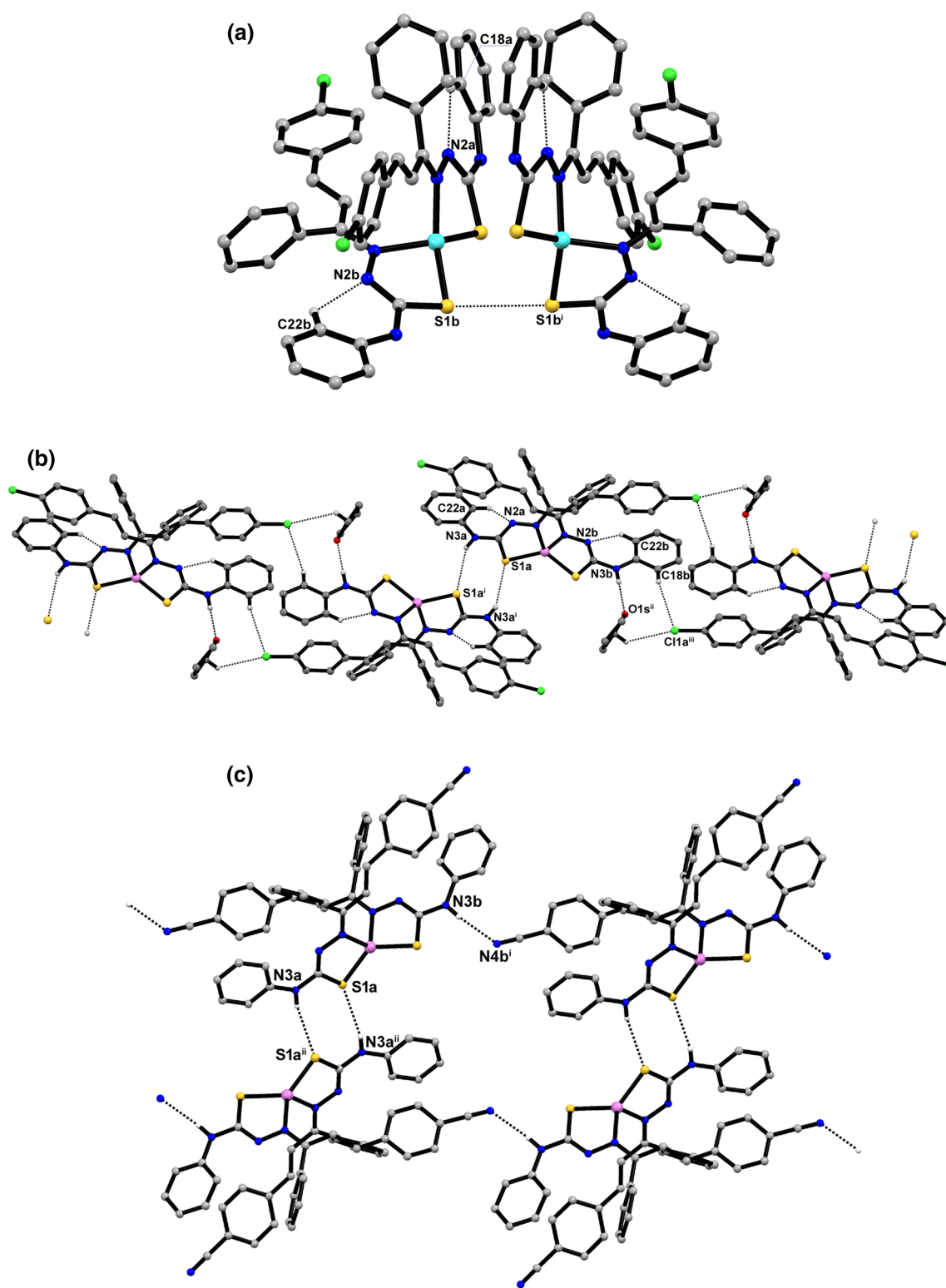


Fig. 3 Details of the crystal packing of compounds **1a**, **1b** and **4b**. Only hydrogen atoms involved in intramolecular and intermolecular contacts are shown

Table 4 Cell viability (%) after 4-h incubation with the compounds at 0.100 mmol L⁻¹ cells (control strain—BY4741)

Compound	Cell viability (%)
Control	100 ± 0.00 ^a
H ₂ O ₂ *	0.0 ± 0.00
HL1	81.33 ± 11.66 ^a
HL3	72.83 ± 8.97 ^a
HL4	53.53 ± 14.21 ^b
1a	97.37 ± 20.86 ^c
3a	81.14 ± 7.95 ^c
4a	66.11 ± 27.66 ^c
1b	92.72 ± 0.00 ^c
3b	80.77 ± 10.44 ^c
4b	77.09 ± 3.49 ^c

Statistical analysis was performed with one-way ANOVA plus Tukey's posttest, with *p* values < 0.05 considered significant

^{a,b,c}Different letters mean statistically different results

*Tested at 1 mM

and *Candida albicans* fungi [32]. Also, some studies have shown that Zn(II) and Cu(II) thiosemicarbazone complexes produce damage in yeast and other cell types [33]. In our case, the complexes exhibited lower toxicity toward *S. cerevisiae*, compared to the free proligands. In addition, no significant difference was observed between the Cu(II) and Zn(II) complexes. Thus, our results indicate that complexation was not effective in increasing the toxicity of the chalcone–thiosemicarbazones against *S. cerevisiae*.

In order to further investigate the proligands, lipid peroxidation assay was performed in the BY4741 strain. **HL1**, **HL3** and **HL4** showed increase in MDA levels (Fig. 4).

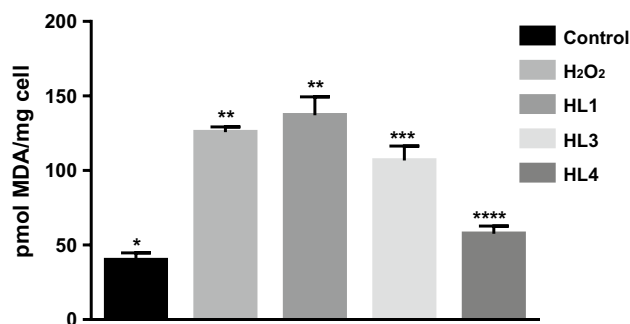


Fig. 4 Effect on lipid peroxidation after 4-h incubation with H₂O₂ and the ligands **HL1**, **HL3** and **HL4** at 0.100 mmol L⁻¹. Lipid peroxidation was measured as pmol of MDA (malondialdehyde) by the method of TBARS (thiobarbituric acid-reactive species). Data represent the means ± SDs of at least three independent experiments (different numbers of asterisks mean statistically different results in each group; *p* < 0.05)

HL1 showed similar toxicity to the positive control (H₂O₂), proving to be more damaging than **HL3** and **HL4**. This result revealed a different profile to that observed in cell viability (Table 4). Both assays have indicated that **HL1** and **HL4** cause damage to yeast cells; however, **HL4** interferes in cell proliferation by preventing formation of viable daughter cells, whereas **HL1** causes lipid peroxidation in the plasma membrane. In this case, it appears that the difference in substituents resulted in different actions on *S. cerevisiae* cells. Other studies have reported thiosemicarbazone derivatives acting in different ways on cellular structures and metabolism, such as antiproliferative activity [34] and redox homeostasis [35]. One of the features of cancer cells is presenting sustained proliferative capacity, which favors tumorigenesis. Thus, therapies that interfere and limit this capacity are desirable, to which compound **HL4** might be a potential alternative to be further evaluated against human cancer cells.

In order to investigate whether coordination interferes in the ability of the proligand to induce plasma membrane damage, **1a** and **1b**—derived from **HL1**—were also evaluated (Fig. 5). The result shows that the Zn(II) complex **1b** has not caused membrane damage, but the Cu(II) complex **1a** revealed a twofold increase in the lipid peroxidation when compared to the control and **1b**, yet induced less damage than **HL1**.

Coordination to Cu(II) and Zn(II) atoms has not led to an increase in membrane damage toward *S. cerevisiae*, when compared to **HL1**, even though **1a** has exhibited some level of lipid peroxidation. According to our results, chalcone–thiosemicarbazones were more toxic to yeast cells than the complexes, with emphasis on **HL4**. On the other hand, the metal complexes caused little toxicity in this cellular model. Considering the potential applicability of Cu(II) and Zn(II) complexes also as antimicrobials, this result may be

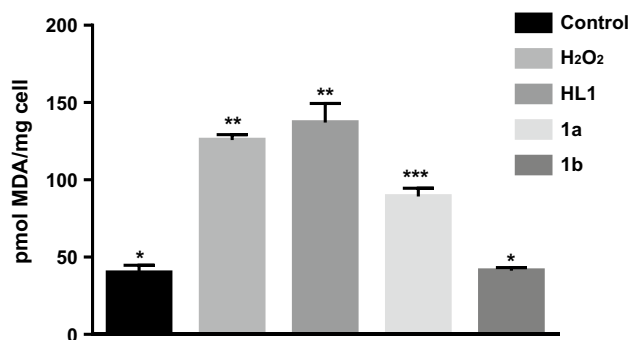


Fig. 5 Lipid peroxidation assay with hydrogen peroxide, **HL1**, **1a** and **1b**. Data represent the means ± SDs of at least three independent experiments (different numbers of asterisks mean statistically different results in each group; *p* < 0.05)

particularly interesting, since this application requires low toxicity to human living cells.

Conclusions

A series of new chalcone–thiosemicarbazone hybrids as well as their Cu(II) and Zn(II) complexes have been obtained and characterized. Spectroscopic analyses revealed that the proligands exist in two tautomeric forms in solution (*E* and *Z* isomers), and upon coordination, the *Z* form is preferential for the complexes. The crystalline structures of two Cu(II) (**1a** and **3a**) and two Zn(II) complexes (**1b** and **4b**) were determined by X-ray diffraction. As expected, the chalcone-TSCs ligands coordinate in the anionic form, through the azomethine nitrogen (N1a and N1b) and the S-thiolate, in a 2:1 ligand:metal proportion, with the metal atom exhibiting a seesaw geometry. Yeast activity demonstrated that the chalcone-TSCs were the most active compounds, especially that containing the cyano substituent, **HL4**. On the other hand, **HL1** (R = Cl) was found to better induce lipid peroxidation among the tested compounds. Coordination with Cu(II) and Zn(II) did not enhance toxicity of the ligands against *S. cerevisiae*. Also, complexes **1a** and **1b** did not induce great levels of membrane damage, even though the Cu(II) complex showed a twofold increase compared to Zn(II). Additional biological investigations are under way in order to evaluate the applicability of the complexes as antimicrobials.

Supplementary data

The CCDC 1835513–1835516 contain the supplementary crystallography data for **1a**, **3a**, **1b** and **4b**. These data can be obtained free of charge via <http://www.ccdc.cam.ac.uk/contents/retrieving.html>, or from the Cambridge Crystallographic Data Centre, 12 Union Road, Cambridge CB2 1EZ, UK; fax: (+44) 1223-336-033; or e-mail: deposit@ccdc.cam.ac.uk.

Acknowledgements The authors thank the Brazilian agencies CAPES, CNPQ and FAPERJ (Grant: Sediadas E-26/010.002894/2014) for financial support, LDRX-UFF (www.ldrx.uff.br/) for the X-ray diffraction analysis and PPGQ-UFRRJ (<http://cursos.ufrrj.br/posgraduacao/ppgq/>) for the facilities.

References

- Beraldo H, Gambino D (2004) The wide pharmacological versatility of semicarbazones, thiosemicarbazones and their metal complexes. *Mini Rev Med Chem* 4:31–39
- Yu Y, Kalinowski DS, Kovacevic Z, Siafakas AR, Jansson PJ, Stefani C, Lovejoy DB, Sharpe PC, Bernhardt PV, Richardson DR (2009) Thiosemicarbazones from the old to new: iron chelators that are more than just ribonucleotide reductase inhibitors. *J Med Chem* 52:5271–5294
- Mendes IC, Moreira JP, Mangrich AS, Balena SP, Rodrigues BL, Beraldo H (2007) Coordination to copper(II) strongly enhances the in vitro antimicrobial activity of pyridine-derived *N*(4)-tolyl thiosemicarbazones. *Polyhedron* 26:3263–3270
- Kovala-Demertzi D, Yadav PN, Wiecek J, Skoulika S, Varadinova T, Demertzi MA (2006) Zinc(II) complexes derived from pyridine-2-carbaldehyde thiosemicarbazone and (1*E*)-1-pyridin-2-ylethan-1-one thiosemicarbazone: synthesis, crystal structures and antiproliferative activity of zinc(II) complexes. *J Inorg Biochem* 100:1558–1567
- Singh P, Anand A, Kumar V (2014) Recent developments in biological activities of chalcones: a mini review. *Eur J Med Chem* 85:758–777
- Verma CP, Kumar KS, Aravindhakshan KK (2017) Synthesis, characterization and pharmacological activity of complexes of Cu(II), Ni(II), Mn(II) and Co(II) from chalcone *N*(4)-methyl(phenyl)thiosemicarbazone. *J Pharm Sci Res* 9:1444–1449
- Zhang HJ, Qian Y, Zhu DD, Yang XG, Zhu HL (2011) Synthesis, molecular modeling and biological evaluation of chalcone thiosemicarbazide derivatives as novel anticancer agents. *Eur J Med Chem* 46:4702–4708
- Da Silva JG, Recio Despaigne AA, Louro SRW, Bandeira CC, Souza-Fagundes EM, Beraldo H (2013) Cytotoxic activity, albumin and DNA binding of new copper(II) complexes with chalcone-derived thiosemicarbazones. *Eur J Med Chem* 65:415–426
- Da Silva JG, Perdigão CCH, Speziali NL, Beraldo H (2013) Chalcone-derived thiosemicarbazones and their zinc(II) and gallium(III) complexes: spectral studies and antimicrobial activity. *J Coord Chem* 66:385–401
- Tan MY, Crouse KA, Ravoof TB, Jotaniand MM, Tiekink ERT (2017) 1-[(*E*)-[(2*E*)-3-(4-Methoxyphenyl)-1-phenylprop-2-en-1-ylidene]amino]-3-phenylurea: crystal structure and Hirshfeld surface analysis. *Acta Crystallogr Sect E* 73:1607–1611
- Tan MY, Crouse KA, Ravoof TB, Tiekink ERT (2015) Crystal structure of 1-[(*Z*)-[(2*E*)-3-(4-chlorophenyl)-1-phenylprop-2-en-1-ylidene]amino]-3-ethylthiourea. *Acta Crystallogr Sect E* 71:1047–1048
- Viñuelas-Zahínos E, Luna-Giles F, Torres-García P, Fernández-Calderón MC (2011) Co(III), Ni(II), Zn(II) and Cd(II) complexes with 2-acetyl-2-thiazoline thiosemicarbazone: synthesis, characterization, X-ray structures and antibacterial activity. *Eur J Med Chem* 46:150–159
- Pahontu E, Julea F, Rosu T, Purcarea V, Chumakov Y, Petrenco P, Gulea A (2015) Antibacterial, antifungal and in vitro antileukemia activity of metal complexes with thiosemicarbazones. *J Cell Mol Med* 19:865–878
- Beckford FA, Webb KR (2017) Copper complexes containing thiosemicarbazones derived from 6-nitropiperonal: antimicrobial and biophysical properties. *Spectrochim Acta A* 183:158–171
- Peycheva E, Alexandrova R, Miloshev G (2014) Application of the yeast comet assay in testing of food additives for genotoxicity. *LWT Food Sci Technol* 59:510–517
- Chandel A, Das KK, Bachhawat AK (2016) Glutathione depletion activates the yeast vacuolar transient receptor potential channel, Yvc1p, by reversible glutathionylation of specific cysteines. *Mol Biol Cell* 27:3913–3925
- Suwito H, Mustofa J, Pudjiastuti P, Fanani MZ, Kimata-Arigo Y, Katahira R, Kawakami T, Fujiwara T, Hase T, Sirat HM, Puspaningsih NNT (2014) Design and synthesis of chalcone derivatives as inhibitors of *Plasmodium falciparum*: pursuing new antimalarial agents. *Molecules* 19:21473–21488
- Reis CM, Sousa-Pereira D, Paiva RO, Kneipp LF, Echevarria A (2011) Microwave-assisted synthesis of new *N*₁-*N*₄-substituted thiosemicarbazones. *Molecules* 16:10668–10684

19. Bruker (2007) APEX2 v2014.5-0. Bruker ASX Inc., Madison
20. Bruker (2013) SAINT v8.34A. Bruker ASX Inc., Madison
21. Sheldrick GM, SADABS (1996) Program for empirical absorption correction of area detector data. University of Göttingen, Göttingen
22. Sheldrick GM (2015) Crystal structure refinement with SHELXL. *Acta Crystallogr Sect C Struct Chem* 71:3–8
23. Dolomanov OV, Bourhis LJ, Gildea RJ, Howard JAK, Puschmann H (2009) COLEX2: a complete structure solution, refinement and analysis program. *J Appl Crystallogr* 42:339–341
24. Macrae CF, Bruno IJ, Chisholm JA, Edgington PR, McCabe P, Pidcock E, Rodriguez-Monge L, Taylor R, van de Streek J, Wood PA (2008) Mercury CSD 2.0: new features for the visualization and investigation of crystal structures. *J Appl Crystallogr* 41:466–470
25. Sadowska-Bartosz I, Paczka A, Molon M, Bartosz G (2013) Dimethyl sulfoxide induces oxidative stress in the yeast *Saccharomyces cerevisiae*. *FEMS Yeast Res* 13:820–830
26. Castro FAV, Mariani D, Panek AD, Eleutherio ECA, Pereira MD (2008) Cytotoxicity mechanism of two naphthoquinones (menadione and plumbagin) in *Saccharomyces cerevisiae*. *PLoS ONE* 3:3999
27. Oliveira RB, Souza-Fagundes EM, Soares RPP, Andrade AA, Krettli AU, Zani CL (2008) Synthesis and antimalarial activity of semicarbazone and thiosemicarbazone derivatives. *Eur J Med Chem* 43:1983–1988
28. Ferraz KSO, Silva NF, Da Silva JG, Speziali NL, Mendes IC, Beraldo H (2012) Structural studies on acetophenone- and benzophenone-derived thiosemicarbazones and their zinc(II) complexes. *J Mol Struct* 1008:102–107
29. García-Tojal J, García-Orad A, Serra JL, Pizarro JL, Lesama L, Arriortua MI, Rojo T (1999) Synthesis and spectroscopic properties of copper (II) complexes derived from thiophene-2-carbaldehyde thiosemicarbazone: structure and biological activity of $[\text{Cu}(\text{C}_6\text{H}_6\text{N}_3\text{S}_2)_2]$. *J Inorg Biochem* 75:45–54
30. Yang L, Powell DR, Houser RP (2007) Structural variation in copper(I) complexes with pyridylmethylamide ligands: structural analysis with a new four-coordinate geometry index, τ_4 . *Dalton Trans* 7:955–964
31. Flores-Huerta AG, Tkatchenko A, Galván M (2016) Nature of hydrogen bonds and S–S interactions in the L-cystine crystal. *J Phys Chem A* 120:4223–4230
32. El-Sharief MAMS, Abbas SY, El-Bayouki KAM, El-Gammal EW (2013) Synthesis of thiosemicarbazones derived from *N*-(4-hippuric acid) thiosemicarbazide and different carbonyl compounds as antimicrobial agents. *Eur J Med Chem* 67:263–268
33. Pahontu E, Fala V, Gulea A, Poirier D, Tapcov V, Rosu T (2013) Synthesis and characterization of some new Cu(II), Ni(II) and Zn(II) complexes with salicylidene thiosemicarbazones: antibacterial, antifungal and in vitro antileukemia activity. *Molecules* 18:8812–8836
34. de Oliveira JF, Lima TS, Vendramini-Costa DB, de Lacerda Pedrosa SCB, Lafayette EA, da Silva RMF, de Almeida SMV, de Moura RO, Ruiz ALTG, de Carvalho JE, de Lima MDCA (2017) Thiosemicarbazones and 4-thiazolidinones indole-based derivatives: synthesis, evaluation of antiproliferative activity, cell death mechanisms and topoisomerase inhibition assay. *Eur J Med Chem* 136:305–314
35. Kalinowski DS, Stefani C, Toyokuni S, Ganz T, Anderson GJ, Subramaniam VN, Trinder D, Olynyk JK, Chu A, Jansson PJ, Sahni S, Lane DJR, Merlot AM, Kovacevic Z, Huang MLH, Lee CS, Richardson D (2016) Redox cycling metals: pedaling their roles in metabolism and their use in the development of novel therapeutics. *Biochim Biophys Acta* 1863:727–748